13th World Conference on Earthquake Engineering
Vancouver, B.C., Canada
August 1-6, 2004
Paper No. 1177

ONLINE DETECTION AND LOCATION OF SEISMIC DAMAGE IN A WATER DISTRIBUTION SYSTEM

Jianwen LIANG[1]

SUMMARY

It is shown that urban water distribution systems can be damaged by strong earthquakes, and the damage cannot easily be detected and located, especially immediately after the earthquakes. In recent years, online damage estimation and diagnosis of buried pipelines attracted much attention of researchers focusing on establishing the relationship between damage ratio (breaks per unit length of pipe) and ground motion with taking the soil condition into consideration. Due to the uncertainty and complexity of the parameters that affect the pipe damage mechanism, it is not easy to estimate the degree of physical damage only with a few numbers of parameters. As an alternative, this paper develops a methodology to detect and locate the seismic damage in a water distribution system by monitoring water pressure online at some selected positions in the water distribution system. For the purpose of online monitoring, emerging supervisory control and data acquisition (SCADA) technology can well be used. A neural network-based inverse analysis method is constructed for detecting the location and extent of damage based on the variation of water pressure. The neural network is trained by using analytically simulated data from the water distribution system with one/multiple damage, and validated by using a set of data that have never been used in the training. It is found that the method provides a quick, effective, and practical way for damage detection and location in a water distribution system.

INTRODUCTION

A water distribution system can be damaged under strong earthquakes, and the damages cannot easily be located, especially immediately after the events, which, on the one hand, always results in water running to waste; and on the other hand, often causes low water pressure or even no water where water is urgently needed. How to solve the problem is crucially significant to post-earthquake emergency response and recovery of an urban water distribution system [1][2].

In recent years, real-time damage estimation and diagnosis of buried pipelines attracted much attention of researchers focusing on establishing the relationship between damage ratio (breaks per unit length of pipes) and ground motion with taking the soil conditions into consideration [3][4][5], and all these studies are based on the starting point that when the damage ratio for a gas distribution system achieves to a prescribed value the gas supply to this distribution system will be shut off. As a macro-damage

[1] Professor, Department of Civil Engineering, Tianjin University, Tianjin 300072, China.
Email: jwliang@tj.cnuninet.net

estimation of a gas distribution system in the stage of post-earthquake emergency response and recovery, damage ratio is a useful index, but it is not appropriate for location of damage in a water distribution system due to the uncertainty and complexity of the parameters that affect the pipe damage mechanism [6]. Eguchi et al [7] put forward a method for damage estimation of a water distribution system, in which, a nominal damage estimated by seismic intensity from earthquake parameters (magnitude, epicentral distance, etc.) is updated gradually through hydraulic analysis based on post-earthquake observation data, but unfortunately, as the authors stated that the updating process is too difficult to realize the tentative idea.

In Tianjin City, China, supervisory control and data acquisition (SCADA) technology has been applied to water distribution systems, in which water pressure and/or flow rate at some selected nodes such as reservoirs, pumps and pipes are monitored online by remote terminal units (RTUs) and the signals are transmitted to main terminal unit (MTU) by radio or internet, as shown in Fig. 1. However, because the number of monitoring stations is limited, and more importantly, there are few effective methodologies available, it is difficult to locate seismic damage precisely and timely in practice.

This paper proposes a methodology to locate seismic damage in a water distribution system by monitoring water pressure variation online at some nodes in the water distribution system. For the purpose of online monitoring, supervisory control and data acquisition (SCADA) technology can well be used. The method is finally validated by examples.

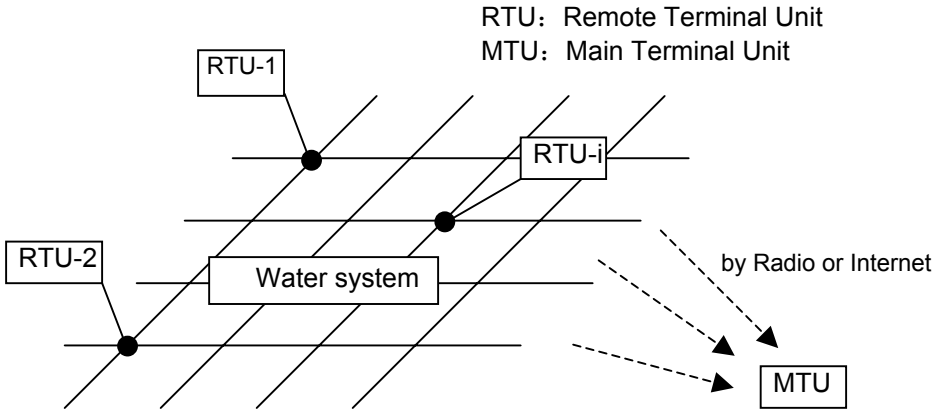

Fig.1: Monitoring of water distribution systems

METHOD

Zoning and monitoring of a water distribution system

A water distribution system is zoned into a few independent sub-systems, where valves are installed among sub-systems. The valves are shut off under normal condition and opened at necessary cases, e.g., an earthquake; one water head monitoring station and one flow rate monitoring station are set up at the intake of one sub-systems, and three water head monitoring stations are installed in the sub-system. The water head and flow rate are monitored and transmitted back by radio or Internet.

Artificial neural network technique

A back-propagation neural network is used in this paper, and the neural network consists of three layers: input, hidden, and output layer. It is shown that one hidden layer is generally sufficient [8].

After input data are fed into the neural network at the input layer, they are propagated through the hidden layer until output data are generated. The output data are then compared with the target output, and an error signal is computed for each output cell. Then the error signals are transmitted backward from the output layer to each cell in the hidden and input layers that contributes directly to the output. This process is repeated until each cell in the network has received an error signal that describes its relative contribution to the total error. Based on the error thus evaluated, connection weights are updated at all cells forcing the network to converge to an acceptable state of performance measured in terms of the root-mean-square (RMS) error.

The sigmoid function is used for output function. In order to normalize the influence of input data with different cells and to prevent the saturation of the output function, in this paper the input and output data are scaled to [-1.0, 1.0] and [0.2, 0.8], respectively, based on the minimums and maximums of the data.

Database development by hydraulic analysis

Using artificial neural network technique to establish the relation between the water head variations at nodes that are not monitored and the water head variations at nodes monitored in a water distribution system, sufficient and well-distributed data for neural network training are needed.

For a given water distribution system, the data can be collected from actual break events or can be simulated by hydraulic analysis or can be the combination of the two ways. For the problem of seismic damage location, it is difficult to obtain sufficient actual data only from break events; therefore, it is necessary to simulate sufficient data anyway. This paper produces all the data by hydraulic analysis.

For a water distribution system at any node i, the continuity condition requires that [9]

$$\sum_j Q_{ij} + Q_{id} + Q_{il} = 0 \tag{1}$$

where Q_{ij} is the flow rate in link ij, Q_{id} is the flow rate of demand at node i, Q_{il} is the flow rate of leakage at node i. Assuming the length and diameter of link ij to be L_{ij} and D_{ij}, respectively, the Hazen-William equation between the head loss H_{ij} and the flow rate Q_{ij} in each link ij can be expressed as

$$Q_{ij} = R_{ij} \left| H_{ij} \right|^{-0.46} H_{ij} \tag{2}$$

where

$$R_{ij} = 0.27853 C_{ij} D_{ij}^{2.63} L_{ij}^{-0.54} \tag{3}$$

$$H_{ij} = E_i - E_j \tag{4}$$

where E_i is the water head at node i, C_{ij} is the roughness coefficient of link ij.

The flow rate of demand Q_{id} at node i is associated with the water head at the node: when the relative water head is not less than a given specific design value (usually the lowest design water head) $H_{\min}$, the flow rate of demand is the normal flow rate Q_{nor}; and when the relative water head is less than $H_{\min}$ but greater than 0, the flow rate [9] is

$$Q_{id} = Q_{nor} (E_i - G_i)^{0.5} H_{\min}^{-0.5} \tag{5}$$

where G_i is the elevation at node i; and when the relative head is less than or equal to 0, the flow rate of demand is 0 at node i.

The flow rate of leakage at node i may be estimated [9]

$$Q_{il} = \begin{cases} d_i (E_i - G_i)^k & (\mathrm{E_i} > G_i) \\ 0 & (\mathrm{E_i} \le G_i) \end{cases} \tag{6}$$

where d_i is the leakage coefficient. In the paper k=1.15. It should be noted that the leakage along all links should be converted into leakage at nodes.

If the number of the nodes is *N*, the following equation is a set of nonlinear equation with *N* unknowns $E_1, E_2, \cdots, E_N$

$$\sum_j R_{ij} \left| E_i - E_j \right|^{-0.46} (E_i - E_j) + Q_{id} + Q_{il} = 0 \tag{7}$$

since Q_{ij}, Q_{id} and Q_{il} all are nonlinear functions of water head.

The Newton-Raphson method is used to solve the nonlinear equation (7). Equation (2) can be written as

$$\begin{aligned} Q_{ij} &= R_{ij} \left| e_i - e_j \right|^{-0.46} (e_i - e_j) + (\partial Q_{ij} / \partial E_i) \Delta E_i + (\partial Q_{ij} / \partial E_j) \Delta E_j \\ &= R_{ij} \left| e_i - e_j \right|^{-0.46} (e_i - e_j) + 0.54 R_{ij} \left| e_i - e_j \right|^{-0.46} (\Delta E_i - \Delta E_j) \end{aligned} \tag{8}$$

Equation (5) can be written as

$$Q_{id} = Q_{nor} (e_i - G_i)^{0.5} H_{\min}^{-0.5} + 0.5 Q_{nor} (e_i - G_i)^{-0.5} H_{\min}^{-0.5} \Delta E_i \tag{9}$$

Equation (6) can be written as

$$Q_{il} = d_i (e_i - G_i)^{1.15} + 1.15 d_i (e_i - G_i)^{0.15} \Delta E_i \tag{10}$$

Substituting equation (8), (9) and (10) into (7), equation (7) can expressed in iterative form

$$\begin{aligned} &\sum_j \{ R_{ij} \left| e_{i,k} - e_{j,k} \right|^{-0.46} (e_{i,k} - e_{j,k}) + 0.54 R_{ij} \left| e_{i,k} - e_{j,k} \right|^{-0.46} (\Delta E_{i,k} - \Delta E_{j,k}) \} \\ &\quad + Q_{nor} (e_{i,k} - G_i)^{0.5} H_{\min}^{-0.5} + 0.5 Q_{nor} (e_{i,k} - G_i)^{-0.5} H_{\min}^{-0.5} \Delta E_{i,k} \\ &\quad + d_i (e_{i,k} - G_i)^{1.15} + 1.15 d_i (e_{i,k} - G_i)^{0.15} \Delta E_{i,k} = 0 \end{aligned} \tag{11}$$

where subscript k indicates the value after k-th iteration.

Staring with the initial value $e_{i,0}$ for E_i ($i = 1,2,...,N$), a set of linear equation (11) is solved for $\Delta E_{i,0}$, thus getting the first iterative results $e_{i,1} = e_{i,0} + \Delta E_{i,0}$. The procedure is repeated until $\left| e_{i,k+1} - e_{i,k} \right|$ ($i = 1,2,...,N$) less than a given specific small value, then $E_i = e_{i,k+1}$ may be considered as the solution at node i.

When a break is occurred to a pipe in a water distribution system, water is discharged at the break. A break can be various shapes and different extents, but all can be expressed as the size of the opening area. The discharge flow rate at a break may be estimated by [10]

$$q_d = C_d A_d \sqrt{2gH} \tag{12}$$

where C_d is the discharge coefficient associated with the break shape, A_d is the opening area, H is the water head at the break, g is the acceleration of gravity. By adjusting the discharge coefficient, various openings can be simulated.

In the same way, equation (12) can be written as

$$q_d = C_d A_d \sqrt{2g} (e_i - G_i')^{0.5} + 0.5 C_d A_d \sqrt{2g} (e_i - G_i')^{-0.5} \Delta E_i \tag{13}$$

where G_i' is the elevation of the opening.

EXAMPLES

Fig. 2 shows a water distribution system with one source, 30 nodes and 50 links. The length and diameter of pipe links are listed in Table 1. It is assumed that the roughness coefficients for all links are 140, the demand flow rates are uniformly distributed with 0.05m^3/sec at all nodes, and the leakage coefficients at all nodes are 2.0×10^{-5}. The elevation of all links is 48.0m, and the water head at resource is 100.0m. A pump station is installed at link 51. Three monitoring stations for water head are set up for the water distribution system, which are indicated in the figure.

Example 1: single damage

First, develop neural network training database by hydraulic analysis of the water distribution system with one break. Calculate the water head at all nodes (including three monitoring stations) without any damage and with one break in sequence at the middle of each link. The extent of the damage is described by the ratio (A_d / A_0) of discharge area at the breaks to the cross area of the pipe, and the ratios are chosen as 0.01, 0.02, 0.1, 0.2 and 0.5, respectively, and the discharge coefficient C_d takes the common use value 0.64, then total 250 sets of data for the water head variations can be obtained for 50 links and 5 damage states for each link. The database is not shown here for the limited space. In order to make the 5 damage states well distributed, take the logarithm of the ratios, and then normalize them. Use the 250 sets of data to train the neural network: 3 neural cells at input layer for the water head variations at 3 monitoring stations; 27 cells at output layer for the water head variations at nodes that are not monitored. Fig.3 shows that the neural network tends to converge after 10000 cycles training, and the RMS error is 0.00177 after 100000 cycles training.

Next, test the neural network to see if it can give us the results that we expect. Input the data used for training and Table 2 shows the water head variations at nodes that are not monitored, e.g., nodes A, B, C and D for break (A_d / A_0 =0.1) at link 9, 20, 24, 25, 26, 27, 28, 31 and 42, respectively. The results in Table 2 are the normalized water head variations, and the values in brackets are the relative error with the targets. From the results it is known that the relative errors are very small, with the minimum 0.05% and the maximum 2.83%, and most are below 1%, which shows the neural network training is successful. This may indicate that there indeed exists an inherent relation between water head variations at different nodes in a given water delivery system, which is the key to the methodology, and 3 monitoring stations are sufficient for the purpose of damage location in the example. As the back-propagation neural network technique is based on the decrease of RMS error of all training data, the relative error of water head variation for a specific node varies around the final training error 0.00177.

Input data that have never been used for training to test the neural network. Table 3 and Table 4 show the water head variations at nodes that are not monitored, e.g., nodes A, B, C and D for breaks A_d / A_0 =0.05 and A_d / A_0 =0.15 at link 9, 20, 24, 25, 26, 27, 28, 31 and 42, respectively. As above the results in Table 3 and Table 4 are the normalized water head variations, and the values in brackets are the relative error with the targets. From these results it is known that the relative errors are larger than those in Table 2, and the maximums are 9.03% and 9.41% for Table 3 and Table 4, respectively, but most are below 5%. This is due to that for the data that have not been used for training the neural network gives the interpolations, and their precisions depend on the RMS error and the distance away from the training data, and the errors tend to the largest at the middle of two training data. Table 3 and Table 4 further show that there indeed exists the inherent relation between water head variations at different nodes in a given water delivery system, and further proves the methodology: the water head variations at 27 nodes (that are not monitored in the paper) can well be predicted from the water head variations at 3 nodes (that are monitored in the paper).

Then locate the damage and estimate the extent of the damage. Fig. 4 shows the contour maps of normalized water head variations at all nodes that are not monitored for break A_d / A_0 =0.05 (between 0.02 and 0.1 used for training) at link 28, which are corresponding to the maximal relative error 9.03% in Table 3. In Fig. 4, the upper figure (a) is the target water head variations contour map, and the lower figure (b) is the diagnosed water head variations contour map. From these contour maps, the diagnosed water head variations are in good agreement with the target water head variations, and it is easy to locate the damage: at the position ⊕ with maximal water head variation, i.e., at link 28, and to estimate the extent of the damage: the maximal value of water head variation $0.02< A_d / A_0 <0.1$.

Fig. 5 shows the contour maps of normalized water head variations at all nodes that are not monitored for break A_d / A_0 =0.15 at link 28, and again the diagnosed water head variations are in good agreement with the target water head variations, and it is easy to locate the damage: at the position ⊕ with maximal water head variation, i.e., at link 28, and it is also easy to know the extent of the damage: the maximal value of water head variation $0.1< A_d / A_0 <0.2$.

As for Fig. 6 and Fig. 7, in the same way, it is easy to locate the damage (link 42), and to estimate the extent of the damage ($0.02< A_d / A_0 <0.1$ and $0.1< A_d / A_0 <0.2$, respectively).

From the above results, it can be concluded that the neural network can accurately locate the damage and estimate the extent of the damage, which may again indicate that there indeed exists an inherent relation between water head variations at different nodes for a given water distribution system, which is the key to the methodology; and which may also indicate that 3 monitoring stations are sufficient for the purpose of damage location.

Example 2: multiple damage

When a water distribution system is subjected to an earthquake, there may be multiple damage. Take the case of two breaks for example for the purpose of demonstration. Assume that there are two breaks at any two different pipe links; and as in the above example, the damage ratios (A_d / A_0) are chosen as 0.01, 0.02, 0.1, 0.2 and 0.5, respectively. In this example, the pump station is considered in the way that the pump is started when the water head is lower than 53m, and the lift of the pump is 10m. Then in the same procedure, train the neural network using the data developed by hydraulic analysis: 3 neural cells at input layer for the water head variations at 3 monitoring stations; 27 cells at output layer for the water head variations at nodes that are not monitored.

Fig. 8 and Fig. 9 show the location of damage and estimation of the extents of the damages at link 28 and link 42 for A_d / A_0 =0.05 and 0.15, respectively. The upper figures (a) are the target water head variations contour maps, and lower figures (b) are the diagnosed water head variations contour maps. The diagnosed water head variations are in good agreement with the target water head variations, and it is easy to locate the damage: at the position ⊕ with peak water head variations, i.e., at link 28 and link 42, and to estimate the extents of the damage, i.e., the peak value of water head variations: $0.02< A_d / A_0 <0.1$ and $0.1< A_d / A_0 <0.2$, respectively.

CONCLUSIONS

This paper proposes a methodology to locate seismic damage in a water distribution system by monitoring water head online at three nodes in the water distribution system, in which, a artificial neural network-based inverse analysis method is developed to estimate the water head variations at all nodes that are not monitored based on the water head variations at the nodes monitored. It is found that the

methodology provides a quick, effective, and practical way in which seismic damage in a water distribution system can be located.

The methodology has the following advantages. First, the method deals with the problem from the point of systems. For a given water distribution system, any break at pipe links or nodes will affect the water head at all other links or nodes; and the different extents of the break will result in different effects; and the same break will bring different effects for links or nodes at different positions. Based on this principle, this paper proposes to locate damages in a water distribution system by monitoring the most sensitive parameter for damage --- water head variations before and after the event at three nodes, and to establish the relation between the water head variations at the nodes that are not monitored and the water head variations at the nodes monitored. Second, by using artificial intelligence of neural network technique, this relation can be established offline, then once there are damage, and the damage may be located online based on the water head variations only at the monitoring nodes. Depending on the water distribution system, this process may only need several seconds to several minutes. Third, by utilizing its advantage in nonlinear mapping of neural network technique, this relation can be established much more accurately overcoming difficulty of other mathematical methods, e.g., regression analysis, in dealing with strongly nonlinear problem. Fourth, using neural network technique may also use its advantage in error's tolerance to greatly reduce the possibility of mistakes in diagnosis. Finally, using neural network technique can also fully utilize the SCADA technology in urban water distribution systems available. It should be pointed out that the method might also be used for diagnosis of water sources and pumps, etc., and for location of a fire fighting and monitoring of its flow status.

ACKNOWLEDGEMENTS

This work was supported by the National Natural Science Foundation of China under Grant No.59878032 and 50378063.

REFERENCES

1. Liang J. "A decision support system for pre-earthquake planning of lifeline networks." PVP-Vol.340, ASME, 1996; 277-282.
2. Liang J. "A comprehensive framework for post-earthquake rehabilitation plan of lifeline networks." PVP-Vol.340, ASME, 1996; 283-289.
3. Cret L. Yamazaki F, Katayama T. "Earthquake damage estimation and decision analysis for emergency shut-off of city gas networks using fuzzy set theory." International Journal of Structural Safety, 1993; **12**(1): 1-19.
4. Nishio N. "Damage ratio prediction for buried pipelines based on the deformability of pipelines and the non-uniformity of ground." Journal of Pressure Vessel Technology, ASME, 1994; **116**(4): 459-466.
5. Takada S, Ogawa Y. "Seismic monitoring and real time damage estimation for lifelines." Proceedings of 4th U.S. Conference on Lifeline Earthquake Engineering, ASCE, San Francisco, 1995; 224-231.
6. Liang J, Sun S. "Site effects on seismic behavior of pipelines: a review." Journal of Pressure Vessel Technology, ASME, 2000; **122**(4): 469-475.
7. Eguchi RT, Chrostowski JD, Till CW. "A rapid post-earthquake damage detection method for underground lifelines." Proceedings of 3rd U.S. Conference on Lifeline Earthquake Engineering, ASCE, Los Angeles, 1991; 714-724.
8. Freeman JA, Skapura DM. "Neural networks: algorithms, applications, and programming techniques." Reading: Addison-Wesley Publishing Company, 1991.
9. Takakuwa T. "Pipeline network analysis and design." Tokyo: Morikita Publishing Company, 1978.
10. Gupta RS. "Hydrology and hydraulic systems." Englewood Cliffs: Prentice-Hall, 1989.

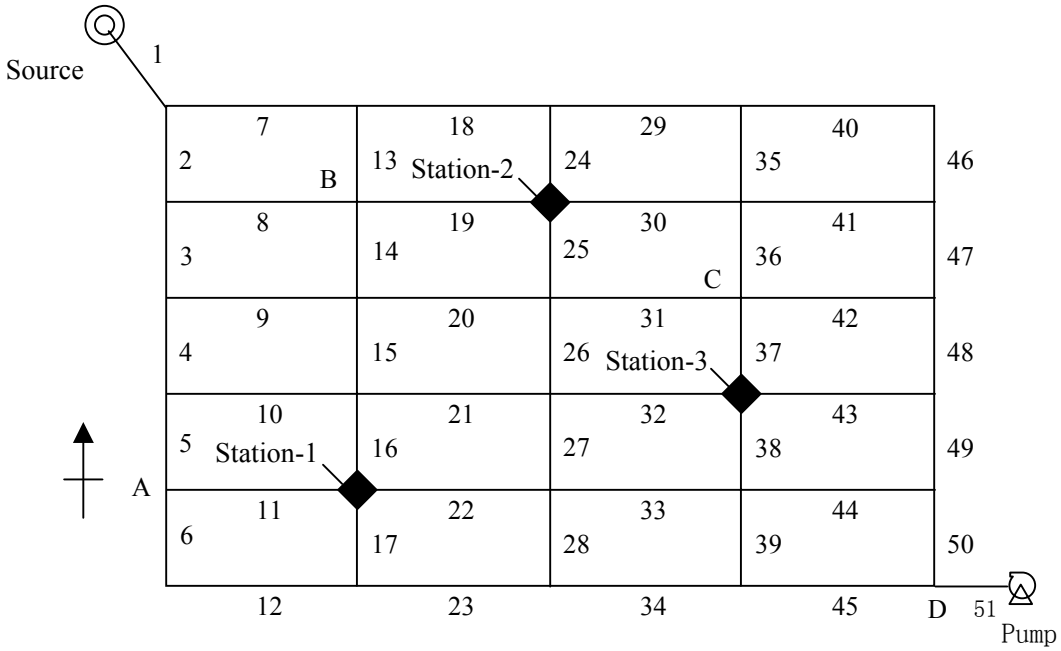

Fig. 2: The example water distribution system with one source, 30 nodes and 51 pipe links, where water head at three nodes are monitored.

Table 1: The diameter and length of pipe links in the example water distribution system.

Link No.	D (m)	L (m)	Link No.	D (m)	L (m)	Link No.	D (m)	L (m)	Link No.	D (m)	L (m)
1	0.80	50	14	0.50	1000	27	0.40	1000	40	0.50	2000
2	0.60	1000	15	0.50	1000	28	0.35	1000	41	0.40	2000
3	0.60	1000	16	0.40	1000	29	0.50	2000	42	0.40	2000
4	0.50	1000	17	0.40	1000	30	0.50	2000	43	0.35	2000
5	0.50	1000	18	0.60	2000	31	0.40	2000	44	0.35	2000
6	0.40	1000	19	0.50	2000	32	0.40	2000	45	0.30	2000
7	0.60	2000	20	0.50	2000	33	0.35	2000	46	0.40	1000
8	0.60	2000	21	0.40	2000	34	0.35	2000	47	0.40	1000
9	0.50	2000	22	0.40	2000	35	0.50	1000	48	0.35	1000
10	0.50	2000	23	0.35	2000	36	0.40	1000	49	0.35	1000
11	0.40	2000	24	0.50	1000	37	0.40	1000	50	0.30	1000
12	0.40	2000	25	0.50	1000	38	0.35	1000			
13	0.60	1000	26	0.40	1000	39	0.35	1000			

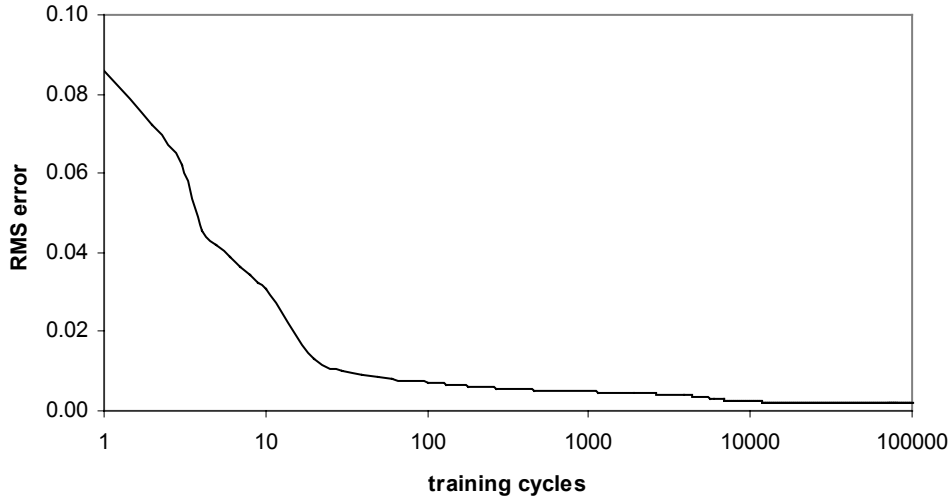

Fig. 3: The training curve of artificial neural network where the RMS error tends to converge after 10000 cycles training, and 0.00177 after 100000 cycles training.

Table 2: The diagnosed water head variations at nodes A, B, C and D that are not monitored for break A_d / A_0 =0.1 at link 9, 20, 24, 25, 26, 27, 28, 31 and 42.

Break at link No.	Water head variation at node A	Water head variation at node B	Water head variation at node C	Water head variation at node D
9	0.5813 (0.41%)	0.4763 (0.13%)	0.5333 (0.39%)	0.5565 (0.80%)
20	0.5753 (0.79%)	0.4832 (0.10%)	0.5805 (0.19%)	0.5857 (0.10%)
24	0.5227 (0.48%)	0.4874 (1.29%)	0.5712 (0.21%)	0.5499 (0.48%)
25	0.5510 (0.56%)	0.4975 (2.83%)	0.5986 (2.18%)	0.5797 (0.05%)
26	0.4682 (0.26%)	0.3758 (0.66%)	0.4813 (2.36%)	0.4904 (0.22%)
27	0.5125 (0.18%)	0.3731 (0.11%)	0.4696 (0.06%)	0.5482 (0.59%)
28	0.4612 (0.81%)	0.3297 (0.57%)	0.4049 (0.15%)	0.5086 (1.88%)
31	0.4412 (1.12%)	0.3755 (1.00%)	05141 (2.24%)	0.4796 (0.25%)
42	0.4506 (0.74%)	0.3779 (0.56%)	0.5553 (1.24%)	0.4982 (0.50%)

Table 3: The diagnosed water head variations at nodes A, B, C and D that are not monitored for break A_d / A_0 =0.05 at link 9, 20, 24, 25, 26, 27, 28, 31 and 42.

Break at link No.	Water head variation at node A	Water head variation at node B	Water head variation at node C	Water head variation at node D
9	0.5625 (3.71%)	0.4792 (6.73%)	0.4970 (1.23%)	0.5231 (0.65%)
20	0.5440 (0.13%)	0.4697 (3.16%)	0.5460 (0.22%)	0.5480 (0.24%)
24	0.5057 (3.31%)	0.4944 (8.90%)	0.5416 (0.95%)	0.5215 (1.44%)
25	0.5231 (0.58%)	0.4967 (8.85%)	0.5608 (0.32%)	0.5422 (0.17%)
26	0.4346 (2.05%)	0.3802 (5.26%)	0.4538 (2.12%)	0.4578 (1.29%)
27	0.4927 (2.26%)	0.3608 (1.32%)	0.4443 (0.05%)	0.5056 (1.27%)
28	0.4399 (1.59%)	0.3306 (3.60%)	0.3882 (0.54%)	0.5132 (9.03%)
31	0.4160 (1.61%)	0.3564 (1.57%)	0.4785 (3.24%)	0.4459 (1.35%)
42	0.4186 (1.23%)	0.3487 (2.84%)	0.5044 (4.36%)	0.4576 (3.09%)

Table 4: The diagnosed water head variations at nodes A, B, C and D that are not monitored for the break A_d / A_0 =0.15 at link 9, 20, 24, 25, 26, 27, 28, 31 and 42.

Break at link No.	Water head variation at node A	Water head variation at node B	Water head variation at node C	Water head variation at node D
9	0.6139 (0.23%)	0.4952 (1.43%)	0.5670 (0.11%)	0.5924 (0.50%)
20	0.6200 (0.60%)	0.5278 (3.49%)	0.6095 (1.41%)	0.6249 (0.27%)
24	0.5459 (0.89%)	0.4701 (7.55%)	0.6031 (0.84%)	0.5751 (0.91%)
25	0.5932 (0.88%)	0.5593 (9.41%)	0.6426 (1.12%)	0.6169 (0.21%)
26	0.5102 (3.07%)	0.4107 (3.87%)	0.5122 (3.23%)	0.5208 (0.33%)
27	0.4962 (8.33%)	0.3554 (8.68%)	0.4809 (2.97%)	0.5369 (7.08%)
28	0.4889 (1.45%)	0.3489 (1.39%)	0.4294 (1.06%)	0.5142 (2.52%)
31	0.4840 (3.09%)	0.4188 (5.62%)	0.5535 (0.65%)	0.5222 (3.45%)
42	0.4781 (1.57%)	0.4036 (2.80%)	0.6025 (0.89%)	0.5445 (2.87%)

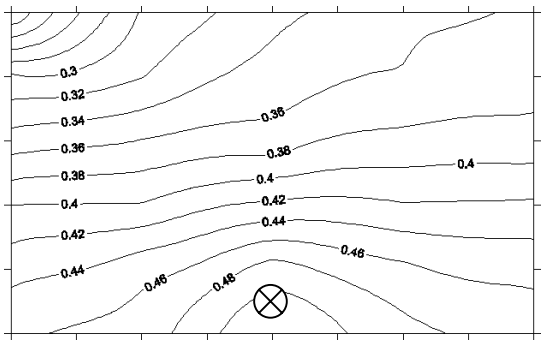

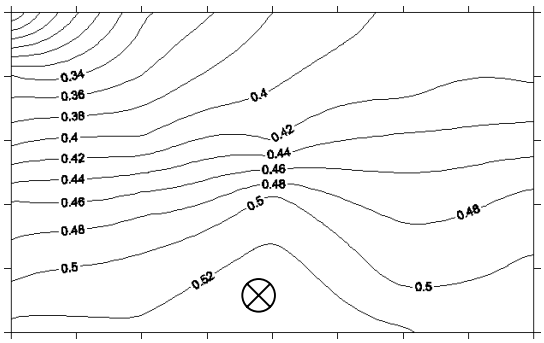

Fig. 4: Location of damage at link 28 for A_d / A_0 =0.05.

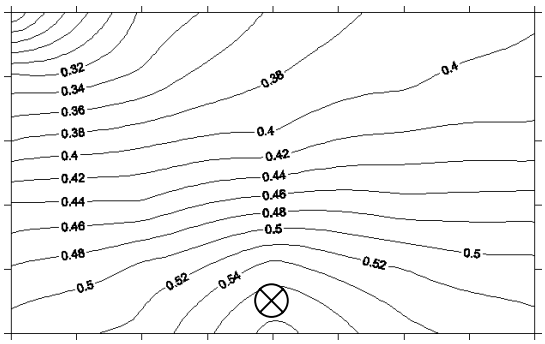

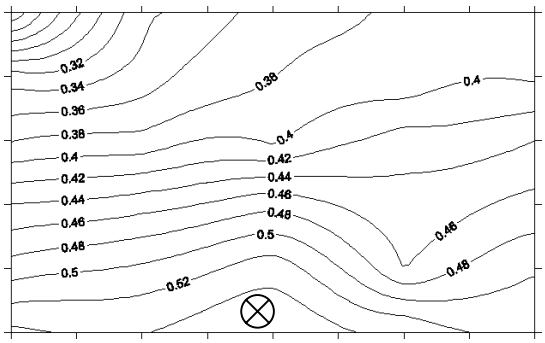

Fig. 5: Location of damage at link 28 for A_d / A_0 =0.15.

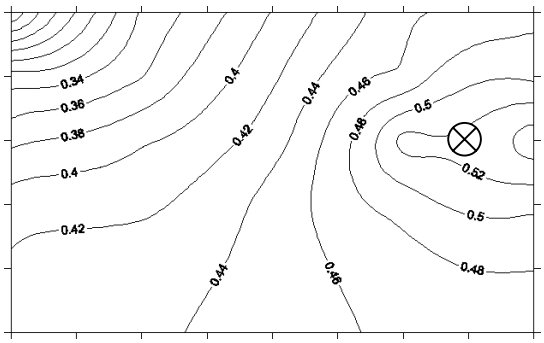

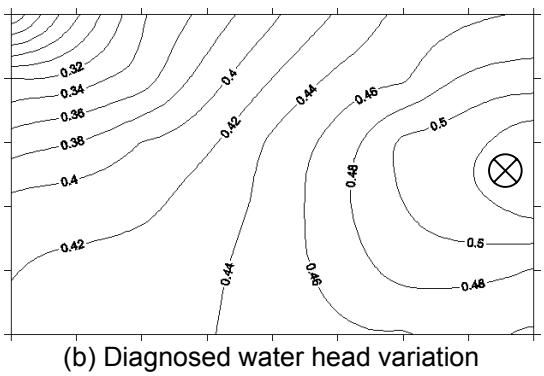

Fig. 6: Location of damage at link 42 for A_d / A_0 =0.05.

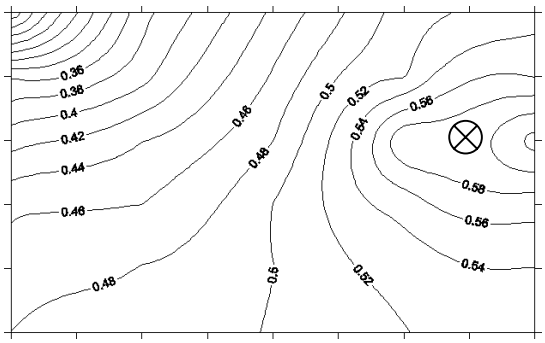

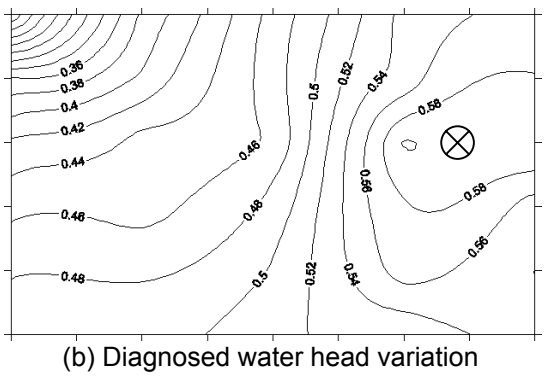

Fig. 7: Location of damage at link 42 for A_d / A_0 =0.15.

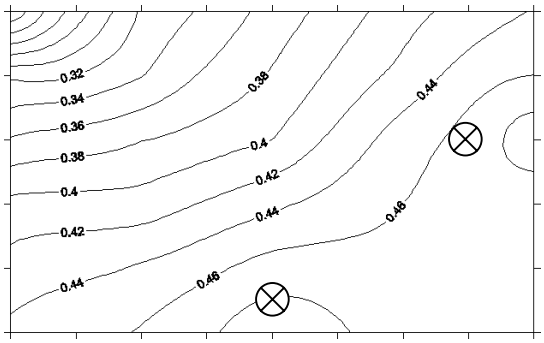

(a) Target water head variation

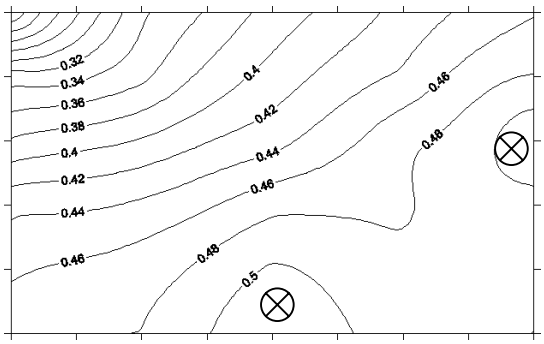

(b) Diagnosed water head variation

Fig. 8: Location of damage at link 28 and link 42 for A_d / A_0 =0.05.

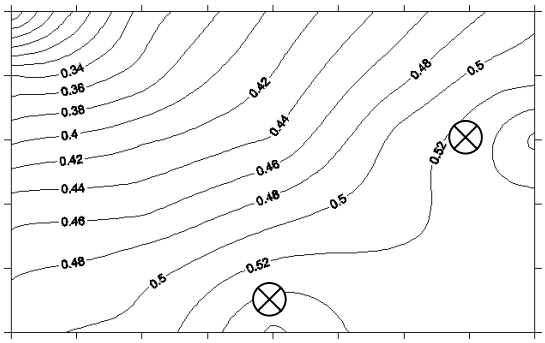

(a) Target water head variation

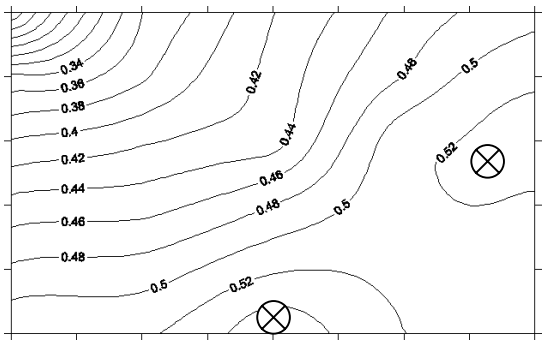

(b) Diagnosed water head variation

Fig. 9: Location of damage at link 28 and link 42 for A_d / A_0 =0.15.